Title
Alblating N-acetylaspartate prevents leukodystrophy in a Canavan disease model

Author
Pleasure, David

Publication Date
2015

Peer reviewed

Brief Communication

Ablating N-acetylaspartate prevents leukodystrophy in a Canavan disease model

Authors: Fuzheng Guo PhD[1*], Peter Bannerman PhD[1*], Emily Mills Ko PhD[1], Laird Miers[1], Jie Xu PhD[1], Travis Burns[1], Shuo Li[2], Ernest Freeman PhD[2], Jennifer A. McDonough PhD[2], and David Pleasure MD[1]

Author Affiliations: [1] Institute for Pediatric Regenerative Medicine, UC Davis School of Medicine and Shriners Hospitals for Children Northern California; [2] Department of Chemistry and Biochemistry, Kent State University

* = Co-First Authors

Corresponding author: David Pleasure MD

Corresponding author's address: UC Davis School of Medicine, c/o Shriners Hospital, 2425 Stockton Boulevard, Sacramento CA 95817

Corresponding author's phone and fax: phone 916-453-2331, FAX 916-453-2288

Corresponding author's e-mail address: david.pleasure@ucdmc.ucdavis.edu

Running head: NAA in a Canavan disease model

Number of words in abstract: 56

Number of words in main text: 1306

Number of figures: 3

Number of tables: 0

Acknowledgement statement: No conflicts of interest by any of the authors. Supported by Shriners Hospitals for Children and the European Leukodystrophy Association.

This article has been accepted for publication and undergone full peer review but has not been through the copyediting, typesetting, pagination and proofreading process which may lead to differences between this version and the Version of Record. Please cite this article as an 'Accepted Article', doi: 10.1002/ana.24392

ABSTRACT

Canavan disease is caused by inactivating aspartoacylase (*ASPA*) mutations that prevent cleavage of N-acetyl-L-aspartate (NAA), resulting in marked elevations in CNS NAA and progressively worsening leukodystrophy. We now report that ablating NAA synthesis by constitutive genetic disruption of N-acetyltransferase-8 like (*Nat8l*) permits normal central nervous system myelination and prevents leukodystrophy in a murine Canavan disease model.

INTRODUCTION

Canavan disease is a recessively inherited spongiform leukodystrophy caused by deficiency of functional aspartoacylase (ASPA).[1,2] N-acetyl-L-aspartate (NAA) is synthesized in neurons from acetyl-CoA and aspartate by N-acetyltransferase-8 like (*NAT8L*, EC 2.3.1.17),[3,4] and then cleaved to acetate and aspartate by oligodendroglial *ASPA* (EC 3.5.1.15).[5] Mammalian CNS NAA is normally maintained at approximately 10mM, but is substantially higher in the ASPA-deficient brain.[6] Radiotracer studies have shown that oligodendroglia use NAA-derived acetate as a precursor for lipogenic acetyl-CoA,[7] and brain acetate and acetyl-CoA levels have been reported to be diminished in mice lacking functional *Aspa* alleles.[8,9] These observations suggested the hypothesis that impaired myelination in Canavan disease is attributable to oligodendroglial deficiency of acetate and acetyl-CoA required for myelin lipid synthesis.[7] An alternative hypothesis, supported by the prominence of astroglial swelling and vacuolation in ASPA-deficient brains[1], and the expression by rodent astroglia of *Nadc3* (*Slc13a3*), a Na^+-coupled plasma membrane dicarboxylate transporter with high NAA affinity,[10] is that leukodystrophy in Canavan disease is a consequence of a deleterious effect of elevated brain NAA, perhaps due to osmotic disequilibrium.[11]

We reasoned that preventing NAA synthesis by disrupting both alleles of *Nat8l* in mice would be an efficient means for evaluating both the “oligodendroglial acetate/acetyl-CoA starvation” and “elevated NAA osmotic toxicity” hypotheses. If oligodendroglial acetate/acetyl-CoA starvation attributable to oligodendroglial inability to derive acetate from NAA is responsible for leukodystrophy in CNS that is deficient in ASPA enzymatic activity, it

would be predicted that the absence of NAA would inhibit CNS myelination in mice with normal *Aspa* alleles, but would neither exacerbate nor prevent leukodystrophy in mice in which both *Aspa* alleles have been mutated to block translation of functional ASPA. If, instead, leukodystrophy in ASPA-deficient mice is attributable to a toxic effect of elevated CNS NAA, it would be predicted that absence of NAA would prevent leukodystrophy in these ASPA-deficient mice.

MATERIALS AND METHODS

Constitutive *Nat8l* knockout (*Nat8l*^{KO}) mice were from the UC Davis KOMP Repository (Project ID VG11213), and *Aspa*^{nur7} mice[6] were from the Jackson Laboratory (Stock Number: 008607). The mice were maintained on a C57BL/6J background, and genotyped by PCR. *Nat8l*$^{KO/KO}$, Aspa$^{nur7/nur7}$, and double homozygous *Nat8l*$^{KO/KO}$/*Aspa*$^{nur7/nur7}$ mice were bred by heterozygous matings, and offspring were obtained in expected Mendelian ratios. Both male and female mice were used in all studies. Motor function was tested by measuring accelerating rotarod retention times (starting speed 4.0 rotations per minute (rpm), speed step 1.3 rpm every 10 seconds). For this purpose, 5 minute training sessions were repeated daily for 10 days, at which point plateau performances had been achieved and were recorded. At the time of sacrifice, mice were deeply anesthetized with ketamine/xylazine prior to euthanasia by decapitation and brain flash freezing (for biochemical studies) or by cardiac perfusion (for histological studies). These procedures were conducted in accord with a UC Davis IACUC-approved protocol. NAA was extracted from whole brain (including cerebellum) and assayed by ^{1}H-magnetic resonance spectroscopy (^{1}H-MRS)[12]. A spectrophotometric method was used to assay acetate in whole brain (including cerebellum).[13] Immunohistology was performed with first antibodies against myelin basic protein (mouse anti-MBP IgG2b, Covance SMI-99P, 1:1000) and glial fibrillary acidic protein (mouse anti-GFAP IgG1, Millipore MAB360, 1:400), and imaged by laser scanning confocal microscopy. Transmission electron microscopy (TEM) was performed on EPON-embedded tissues.

RESULTS

Nat8l$^{KO/KO}$ mice—Both male and female adult homozygous constitutive *Nat8l* knockout (*Nat8l*$^{KO/KO}$) mice were, on average, 20% heavier than littermate wild-type (*Nat8l*$^{WT/WT}$) mice of the same sex, but were otherwise clinically undistinguishable from adult N*at8l*$^{WT/WT}$ mice. Brain NAA was not detectable in the *Nat8l*$^{WT/WT}$ mice by ^{1}H-MRS (**Figure 1A**). TEM demonstrated intact CNS myelination in the N*at8l*$^{KO/KO}$ mice; linear regression analysis of myelin G-ratios of 3 p60 *Nat8l*$^{WT/WT}$ control vs 3 p60 *Nat8l*$^{KO/KO}$ mice showed a slightly lower G ratio (ie, thicker myelin) in *Nat8l*$^{KO/KO}$ corpus callosum (G-ratio intercept 0.6392, SEM=0.0145) than in *Nat8l*$^{WT/WT}$ corpus callosum (G-ratio intercept 0.6601, SEM=0.0081) ($p<0.01$, Student's 2-tailed t-test). However, linear regression analysis of dorsal corticospinal tract G-ratios in the same mice showed no significant differences between the two groups (data not shown). Higher magnification TEMs showed myelin lamellar thickness did not differ significantly between the *Nat8l*$^{KO/KO}$ and *Nat8l*$^{WT/WT}$ mice (data not shown).

Aspa$^{nur7/nur7}$ mice--As previously reported[6], ataxia appeared a few weeks post-weaning in *Aspa*$^{nur7/nur7}$ mice, and worsened progressively thereafter. In addition, short generalized seizures were often seen in these homozygous *Aspa* mutant mice as they aged. Brain NAA concentrations in *Aspa*$^{nur7/nur7}$/*Nat8l*$^{WT/WT}$ mice were approximately two-fold higher than in littermate *Aspa*$^{WT/WT}$/*Nat8l*$^{WT/WT}$ mice (**Fig. 1A**). Accelerating rotarod performance of the *Aspa*$^{nur7/nur7}$*Nat8l*$^{WT/WT}$ mice was markedly impaired (**Fig. 1B**). Astrogliosis, vacuolation, and remyelinating axons were prominent in *Aspa*$^{nur7/nur7}$/*Nat8l*$^{WT/WT}$ cerebellum (**Figs. 2 and 3**) and forebrain (not shown). In wild-type (*Aspa*$^{WT/WT}$/*Nat8l*$^{WT/WT}$) control mice, the brain

acetate concentration was 0.1136 +/- 0.0061 mg/g (mean +/- SEM, n=8), but was diminished by 38% (0.0702 +/- 0.0086 mg/g, n=6, p<0.01) in *Aspa*$^{WT/WT}$/*Nat8l*$^{KO/KO}$ mice, and by 52% (0.0548 +/- 0.0110 mg/g, n=4, p<0.001) in *Aspa*$^{nur7/nur7}$/*Nat8l*$^{WT/WT}$ mice) (one-way ANOVA with Bonferroni's multiple comparison test).

Aspa$^{nur7/nur7}$/*Nat8l*$^{KO/KO}$ mice--Brain NAA was not detectable in *Aspa*$^{nur7/nur7}$/*Nat8l*$^{KO/KO}$ mice (**Fig. 1A**). In contrast to *Aspa*$^{nur7/nur7}$/*Nat8l*$^{WT/WT}$ mice, *Aspa*$^{nur7/nur7}$/*Nat8l*$^{KO/KO}$ mice did not develop ataxia, and their accelerating rotarod performance was normal (**Fig. 1B**). Also in contrast to *Aspa*$^{nur7/nur7}$/*Nat8l*$^{WT/WT}$ mice, immunohistology and transmission electron microscopy showed no evidences of astroglial vacuolation, astrogliosis, or demyelination in *Aspa*$^{nur7/nur7}$/*Nat8l*$^{KO/KO}$ cerebellum (**Figs. 2 and 3**) or forebrain (not shown).

DISCUSSION

The substantial diminutions in brain acetate levels in *Aspa*$^{nur7/nur7}$/*Nat8l*$^{WT/WT}$ mice, in which NAA cannot be cleaved to acetate and aspartate because of the absence of functional *Aspa*, and also in *Aspa*$^{WT/WT}$/*Nat8l*$^{KO/KO}$ mice, in which NAA cannot be synthesized because of the absence of functional *Nat8l*, support one component of the oligodendroglial acetate/acetyl-CoA starvation in Canavan disease hypothesis, by indicating that acetate derived from NAA is important in maintaining a normal brain acetate pool. Additional support for "acetate starvation" in Canavan disease was provided by previous reports that dietary supplements to enhance brain acetyl-CoA supplies diminished the severity of leukodystrophy in ASPA-deficient rodents.[9] But our demonstration that CNS myelination is intact in both *Aspa*$^{WT/WT}$*Nat8l*$^{KO/KO}$ mice, in which NAA cannot be synthesized, and in *Aspa*$^{nur7/nur7}$/*Nat8l*$^{KO/KO}$ mice, in which NAA cannot be cleaved, has substantially weakened this hypothesis. Importantly, *Aspa*$^{nur7/nur7}$ mice were entirely protected against development of leukodystrophy when their capacity to synthesize NAA was ablated by constitutive deletion of *Nat8l*, thus supporting the "elevated NAA osmotic toxicity" hypothesis[11], a conclusion also compatible with the recent report of redistribution of the water channel protein aquaporin 4 in astroglia in *Aspa*$^{nur7/nur7}$ mice.[14]

Though homozygous constitutive deletion of *Nat8l* did not impede accelerating rotarod performance or CNS myelination, abnormal social interactions have been documented in *Nat8l*$^{KO/KO}$ mice,[15] and the single homozygous *NAT8L* mutant human reported thus far was developmentally delayed.[3,16] Those observations suggest that NAA,

though not essential to support myelination, is required for other aspects of normal CNS development.

Since neither *Aspa*$^{nur7/nur7}$ nor *Nat8l*$^{KO/KO}$ mice can employ NAA-derived acetate as a precursor for brain acetyl-CoA, what substrates do they use instead for myelin lipid synthesis? Studies of cultured brown adipocytes which, like neurons, express *Nat8l*, showed that the lipogenic acetyl-CoA pool can be maintained at a normal level in the absence of NAA synthesis by induction of the ATP-citrate lyase pathway, which generates acetyl-CoA from citrate exported from mitochondria,[17] a pathway known to be active in the CNS.[18]

Provision of functional ASPA to brain by viral *Aspa* transduction has been reported to be effective in suppressing leukodystrophy in *Aspa* mutant mice, and to a lesser extent by viral *ASPA* transduction in children with Canavan disease.[19,20] An important implication of the "elevated NAA toxicity" hypothesis is that delivery of functional ASPA to any CNS cells capable of NAA uptake would likely benefit children with Canavan disease by diminishing brain NAA overload. Development of CNS-permeant NAT8L inhibitors, and of methods to accelerate clearance of NAA from the CNS, may also prove useful as adjunctive therapies for Canavan disease.

References

1. Adachi M, Torii J, Schneck L, Volk BW: Electron microscopic and enzyme histochemical studies of the cerebellum in spongy degeneration (van Bogaert and Bertrand type). Acta Neuropath 1972; 20:22-31.

2. Matalon R, Michals K, Sebesta D, et al: Aspartoacylase deficiency and N-acetylaspartic aciduria in patients with Canavan disease. Am J Med Genet 1988; 29:463-471.

3. Wiame E, Tyteca D, Pierrot N, et al: Molecular identification of aspartate N-acetyltransferase and its mutation in hypacetylaspartia. Biochem J 2010; 425:127-136.

4. Ariyannur PS, Moffett JR, Manickam P, et al (2010) Methamphetamine-induced neuronal protein NAT8L is the NAA biosynthetic enzyme: implications for specialized acetyl coenzyme A metabolism in the CNS. Brain Res 2010; 1335:1-13.

5. Francis JS, Strande L, Pu A, Leone P: Endogenous *aspartoacylase* expression is responsive to glutamatergic activity *in vitro* and *in vivo.* Glia 2011; 59:1435-1446.

6. Traka M, Wollmann RL, Cerda SR, et al: *Nur7* is a nonsense mutation in the mouse aspartoacylase gene that causes spongy degeneration of the CNS. J Neurosci 2008; 28:11537-11549.

7. Burri R, Steffen C, Herschkowitz N: N-Acetyl-L-aspartate is a major source of acetyl groups for lipid synthesis during rat brain development. Dev Neurosci 1991; 13:403-412.

8. Madhavarao CN, Arun P, Moffett JR, et al: Defective N-acetylaspartate catabolism reduces brain acetate levels and myelin lipid synthesis in Canavan's disease. Proc Natl Acad Sci USA 2005; 102:5221-6.

9. Francis JS, Markov V, Leone P: Dietary triheptanoin rescues oligodendrocyte loss, dysmyelination and motor function in the nur7 mouse model of Canavan disease. J Inherit Metab Dis 2014; 37:369-381.

10. Yodoya E, Wada M, Shimada S, et al: Functional and molecular identification of sodium-coupled dicarboxylate transporters in rat primary culture cerebrocortical astrocytes and neurons. J Neurochem 2006; 97:162-173.

11. Baslow MH, Guilfoyle DN: Canavan disease, a rare early-onset human spongiform leukodystrophy: insights into its genesis and possible clinical interventions. Biochimie 2013; 95:946-956.

12. Le Belle JE, Harris NG, Williams SR, Bhakoo KK: A comparison of cell and tissue extraction techniques using high-resolution ^{1}H-NMR spectroscopy. NMR Biomed 2002; 15:37-44.

13. Li S, Clements R, Sulak M, et al: Decreased NAA in gray matter is correlated with decreased availability of acetate in white matter in postmortem multiple sclerosis cortex. Neurochem Res 2013; 38:2385-2396.

14. Clarner T, Wieczorek N, Krauspe B, et al: Astroglial redistribution of aquaporin 4 during spongy degeneration in a Canavan disease mouse model. J Mol Neurosci 2013; 53:22-30.

15. Furukawa-Hibi Y, Nitta A, Fukumitsu H, et al: Absence of SHATI/Nat8l reduces social interaction in mice. Neurosci Lett 2012; 526:79-84.

16. Martin E, Capone A, Schneider J, et al: Absence of N-acetylaspartate in the human brain: impact on neurospectroscopy? Ann Neurol 2001; 49:518-521.

17. Pessenthener AR, Pelzmann HJ, Walenta E, et al: NAT8L (N-acetyltransferase 8-like) accelerates lipid turnover and increases energy expenditure in brown adipocytes. J Biol Chem 2013; 268:36040-36051.

18. Szutowicz A, Lysiak W: Regional and subcellular distribution of ATP-citrate lyase and other enzymes of acetyl-CoA metabolism in rat brain. J Neurochem 1980; 35:775-785.

19. Leone P, Shera D, McPhee SWJ, et al: Long-term follow-up after gene therapy for Canavan disease. Science Trans Med 2012; 4:165ra163.

20. Kantor B, McCown T, Leone P, Gray SJ: Clinical applications involving CNS gene transfer. Advances in Genetics 2014; 87:71-124.

FIGURE LEGENDS

Figure 1. (**A**) Brain NAA concentrations were more than two-fold higher in p60 Aspa$^{nur7/nur7}$/*Nat8l*$^{WT/WT}$ mice than in p60 littermate control *Aspa*$^{WT/WT}$/*Nat8l*$^{WT/WT}$ mice, but NAA was not detectable in the brains of either *Aspa*$^{WT/WT}$/*Nat8l*$^{KO/KO}$ or *Aspa*$^{nur7/nur7}$/*Nat8l*$^{KO/KO}$ mice. (**B**) In comparison to p60 *Aspa*$^{WT/WT}$/*Nat8l*$^{WT/WT}$ normal control mice (2 females, 3 males), accelerating rotarod performance was substantially diminished in p60 *Aspa*$^{nur7/nur7}$/*Nat8l*$^{WT/WT}$ mice (4 females, 2 males). Accelerating rotarod performances of p60 *Aspa*$^{WT/WT}$/*Nat8l*$^{KO/KO}$ mice (2 females, 4 males) and of p60 *Aspa*$^{nur7/nur7}$/*Nat8l*$^{KO/KO}$ mice (5 females, 5 males) did not differ significantly from those of normal control mice. Vertical bars denote SEMs; statistical analysis in both Panel A and Panel B was by one-way ANOVA with Bonferroni's multiple comparison post-test. n.s = not significantly different. * = $p<0.05$, **=$p<0.01$, ***=$p<0.001$.

Figure 2. (**A**) An 0.5um confocal optical slice of cerebellar white matter from a p60 *Aspa*$^{nur7/nur7}$/*Nat8l*$^{WT/WT}$ mouse, immunostained for glial fibrillary acidic protein (GFAP, green) and myelin basic protein (MBP, red), showing small and large vacuoles (v) apparently lined by GFAP. Size bar = 10um. (**B**) TEM of cerebellar white matter from a p60 Aspa$^{nur7/nur7}$/*Nat8l*$^{WT/WT}$ mouse. A=astrocyte nucleus. Remyelinating axon is indicated by an arrow. Size bar = 2um. (**C**) TEM showing cerebellar gray matter vacuolation in a p60 *Aspa*$^{nur7/nur7}$/*Nat8l*$^{WT/WT}$ mouse (center panel) which was not present in a p60 *Aspa*$^{WT/WT}$/*Nat8l*$^{WT/WT}$ control mouse (left panel) or a p60 *Aspa*$^{nur7/nur7}$/*Nat8l*$^{KO/KO}$ mouse

(right panel). P=Purkinje cell. Straight arrows point to astroglial processes. The curved arrow in the center panel points to a pale astroglial process containing glial filaments. Size bars = 5um. Results shown in Figure 2 were representative of those obtained with 3 mice in each of these 3 genetic groups.

Figure 3: Laser-scanning confocal stack cerebellar images immunostained for MBP (green) (A1,B1,C1) or both MBP (green) and GFAP (red) (A2,B2,C2) showing demyelination, astrogliosis, and vacuolation in a p60 *Aspa*$^{nur7/nur7}$/*Nat8l*$^{WT/WT}$ mouse (B1,C1); these abnormalities were not present in a p60 wild-type (*Aspa*$^{WT/WT}$/*Nat8l*$^{WT/WT}$ control mouse (A1,A2) or a p60 *Aspa*$^{nur7/nur7}$/*Nat8l*$^{KO/KO}$ mouse (C1,C2). All panels in this figure were counterstained with DAPI. Size bars = 5um.

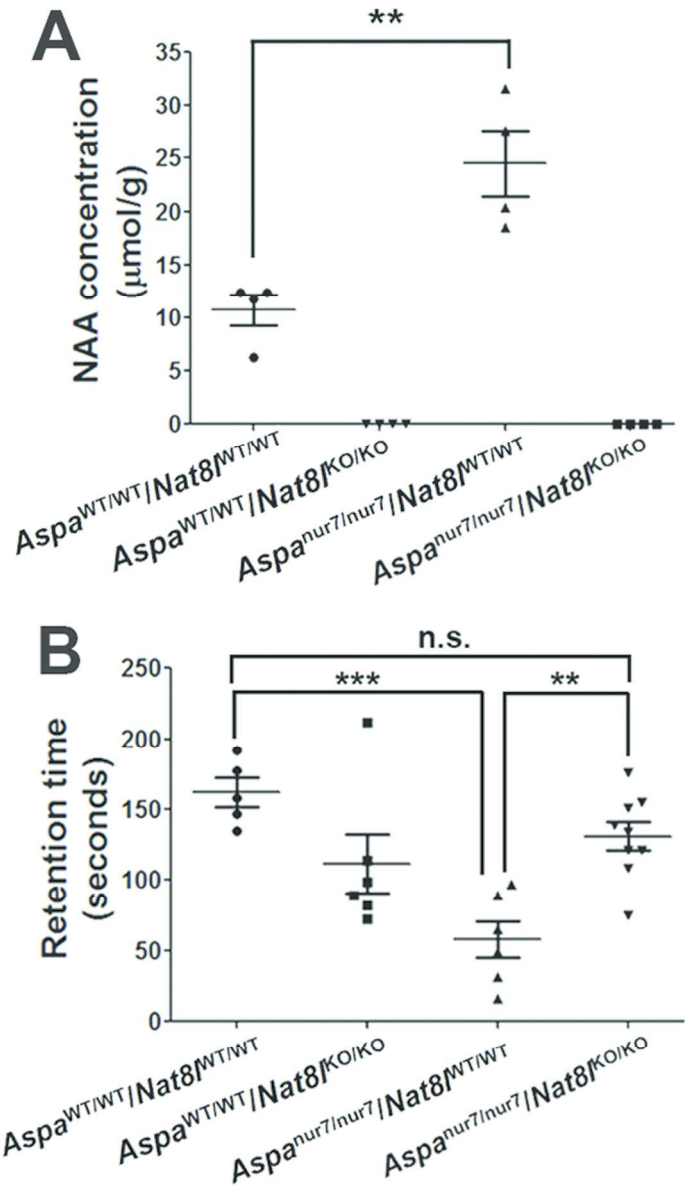

Figure 1. (A) Brain NAA concentrations were more than two-fold higher in p60 Aspanur7/nur7/Nat8lWT/WT mice than in p60 littermate control AspaWT/WT/Nat8lWT/WT mice, but NAA was not detectable in the brains of either AspaWT/WT/Nat8lKO/KO or Aspanur7/nur7/Nat8lKO/KO mice. (B) In comparison to p60 AspaWT/WT/Nat8lWT/WT normal control mice (2 females, 3 males), accelerating rotarod performance was substantially diminished in p60 Aspanur7/nur7/Nat8lWT/WT mice (4 females, 2 males). Accelerating rotarod performances of p60 AspaWT/WT/Nat8lKO/KO mice (2 females, 4 males) and of p60 Aspanur7/nur7/Nat8lKO/KO mice (5 females, 5 males) did not differ significantly from those of normal control mice. Vertical bars denote SEMs; statistical analysis in both Panel A and Panel B was by one-way ANOVA with Bonferroni's multiple comparison post-test. n.s = not significantly different. * = $p<0.05$, **=$p<0.01$, ***=$p<0.001$.
80x139mm (300 x 300 DPI)

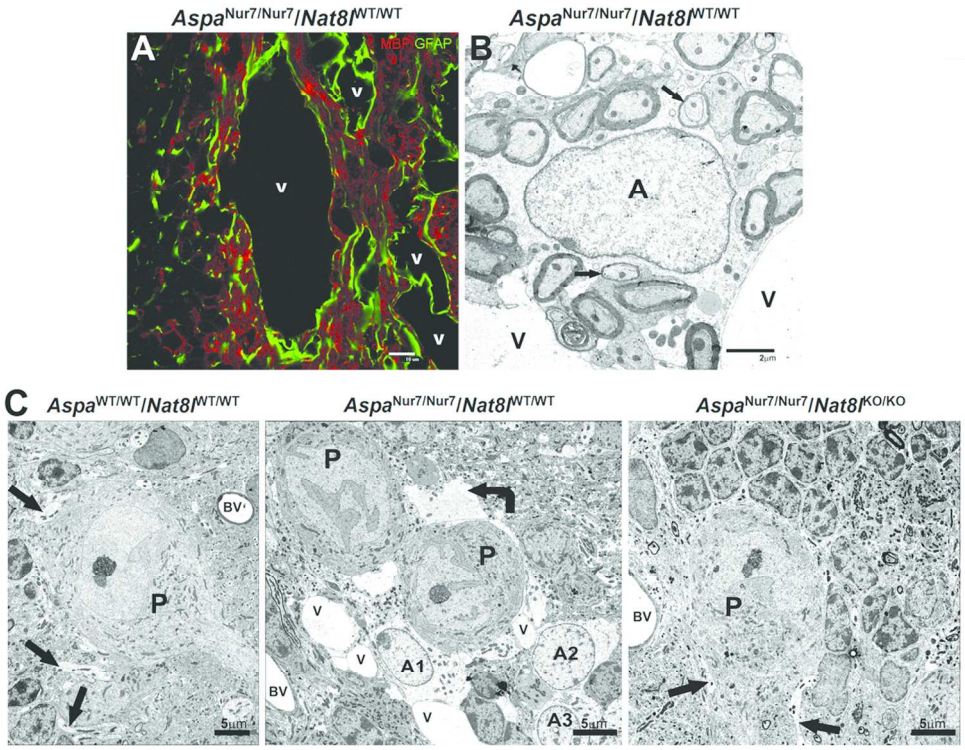

Figure 2. (A) An 0.5um confocal optical slice of cerebellar white matter from a p60 Aspanur7/nur7/Nat8lWT/WT mouse, immunostained for glial fibrillary acidic protein (GFAP, green) and myelin basic protein (MBP, red), showing small and large vacuoles (v) apparently lined by GFAP. Size bar = 10um. (B) TEM of cerebellar white matter from a p60 Aspanur7/nur7/Nat8lWT/WT mouse. A=astrocyte nucleus. Remyelinating axon is indicated by an arrow. Size bar = 2um. (C) TEM showing cerebellar gray matter vacuolation in a p60 Aspanur7/nur7/Nat8lWT/WT mouse (center panel) which was not present in a p60 AspaWT/WT/Nat8lWT/WT control mouse (left panel) or a p60 Aspanur7/nur7/Nat8lKO/KO mouse (right panel). P=Purkinje cell. Straight arrows point to astroglial processes. The curved arrow in the center panel points to a pale astroglial process containing glial filaments. Size bars = 5um. Results shown in Figure 2 were representative of those obtained with 3 mice in each of these 3 genetic groups.
169x130mm (300 x 300 DPI)

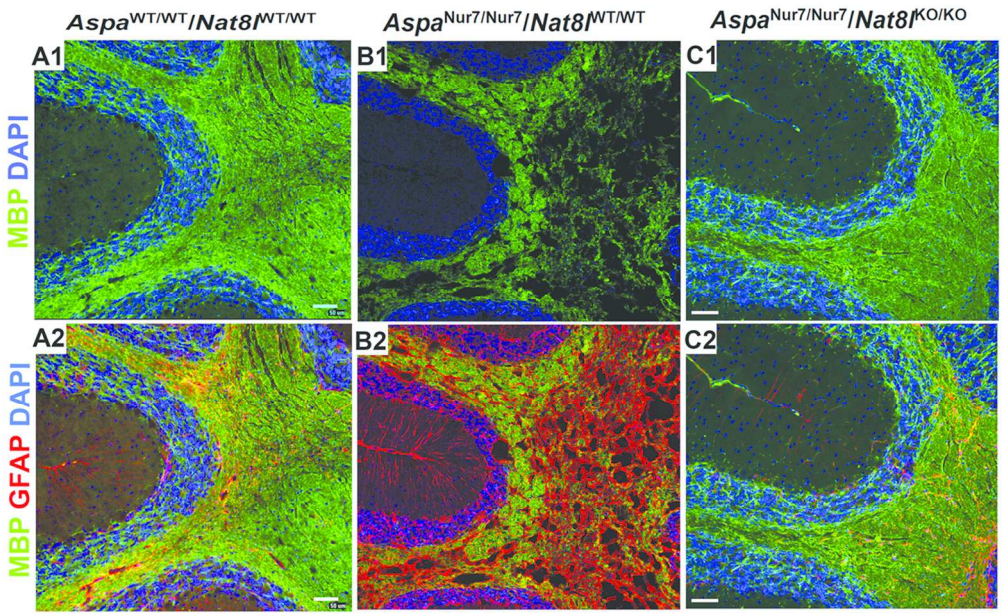

Figure 3: Laser-scanning confocal stack cerebellar images immunostained for MBP (green) (A1,B1,C1) or both MBP (green) and GFAP (red) (A2,B2,C2) showing demyelination, astrogliosis, and vacuolation in a p60 Aspanur7/nur7/Nat8lWT/WT mouse (B1,C1); these abnormalities were not present in a p60 wild-type (AspaWT/WT/Nat8lWT/WT control mouse (A1,A2) or a p60 Aspanur7/nur7/Nat8lKO/KO mouse (C1,C2). All panels in this figure were counterstained with DAPI. Size bars = 5um.
170x106mm (300 x 300 DPI)